Flinders UNIVERSITY

A finite element study on the mechanical response of the head-neck interface of hip implants under realistic forces and moments of daily activities: Part 1, level walking

Hamidreza Farhoudi, Khosro Fallahnezhad, Reza H. Oskouei, Mark Taylor

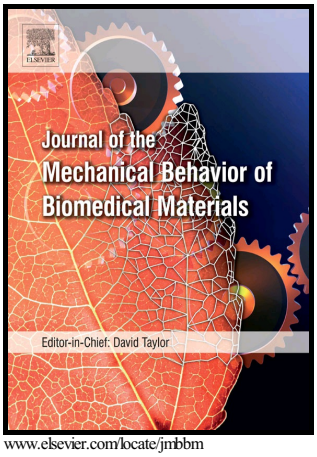

www.elsevier.com/locate/jmbbm

PII: S1751-6161(17)30355-7
DOI: http://dx.doi.org/10.1016/j.jmbbm.2017.08.012
Reference: JMBBM2456

To appear in: *Journal of the Mechanical Behavior of Biomedical Materials*

Received date: 27 February 2017
Revised date: 4 August 2017
Accepted date: 8 August 2017

Cite this article as: Hamidreza Farhoudi, Khosro Fallahnezhad, Reza H. Oskouei and Mark Taylor, A finite element study on the mechanical response of the head-neck interface of hip implants under realistic forces and moments of daily activities: Part 1, level walking, *Journal of the Mechanical Behavior of Biomedical Materials,* http://dx.doi.org/10.1016/j.jmbbm.2017.08.012

A finite element study on the mechanical response of the head-neck interface of hip implants under realistic forces and moments of daily activities: Part 1, level walking

Author 1: Hamidreza Farhoudi
Affiliation: The Medical Device Research Institute, Flinders University, Adelaide, Australia

Author 2: Khosro Fallahnezhad
Affiliation: The Medical Device Research Institute, Flinders University, Adelaide, Australia

Author 3 & Corresponding Author: Reza H Oskouei
Affiliation: The Medical Device Research Institute, Flinders University, Adelaide, Australia
Email: reza.oskouei@flinders.edu.au
Phone: +61-8-82012782

Author 4: Mark Taylor
Affiliation: The Medical Device Research Institute, Flinders University, Adelaide, Australia

Abstract

This paper investigates the mechanical response of a modular head-neck interface of hip joint implants under realistic loads of level walking. The realistic loads of the walking activity consist of three dimensional gait forces and the associated frictional moments. These forces and moments were extracted for a 32 mm metal-on-metal bearing couple. A previously reported geometry of a modular CoCr/CoCr head-neck interface with a proximal contact was used for this investigation. An explicit finite element analysis was performed to investigate the interface mechanical responses. To study the level of contribution and also the effect of superposition of the load components, three different scenarios of loading were studied: gait forces only, frictional moments only, and combined gait forces and frictional moments. Stress field, micro-motions, shear stresses and fretting work at the contacting nodes of the interface were analysed. Gait forces only were found to significantly influence the mechanical environment of the head-neck interface by temporarily extending the contacting area (8.43% of initially non-contacting surface nodes temporarily came into contact), and therefore changing the stress field and resultant micro-motions during the gait cycle. The frictional moments only did not cause considerable changes in the mechanical response of the interface (only 0.27% of the non-contacting surface nodes temporarily came into contact). However, when superposed with the gait forces, the mechanical response of the interface, particularly micro-motions and fretting work, changed compared to the forces only case. The normal contact stresses and micro-motions obtained from this realistic load-controlled study were typically in the range of 0-275 MPa and 0-38 μm, respectively. These ranges were found comparable to previous experimental displacement-controlled pin/cylinder-on-disk fretting corrosion studies.

Graphical abstract

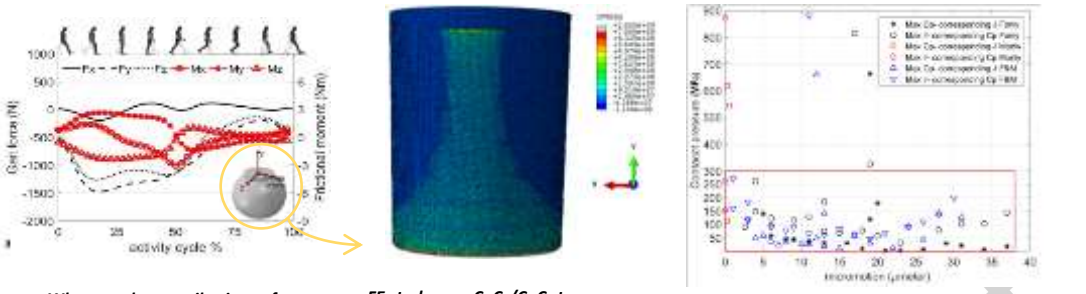

Keywords

Hip implants; Head-neck taper junction; Contact stresses; Micro-motions; Fretting work; Walking.

1. Introduction

Contemporary modular designs of Total Hip Replacement (THR) is a successful solution for surgeons to cope with various anatomies of different patients. Modular THRs also offer the option of replacing only the failed components and keeping the others in place during revision surgeries [1]. In spite of these advantages, modular THRs have suffered from an increasing number of failures which in part are caused by adverse local tissue reaction from metallosis and pseudotumors [2, 3]. Histological studies have shown the presence of corrosion products and metal ions in the local tissues surrounding metallic modular junctions [4-6]. Fretting corrosion is known to occur at the head-neck taper junction of THRs and has been identified as the main cause of metal ion release to the surrounding tissues [7, 8]. Fretting corrosion is understood to be a function of a range of parameters such as loading condition, contact geometry, stress field at the interface, relative micro-motion, characteristics of the contacting materials and corrosivity of the environment [9]. Fretting is identified as the initiator of the fretting corrosion phenomenon also termed as mechanically assisted crevice corrosion in modular junctions [10]. Fretting itself is a function of a variety of parameters, in particular stress field, micro-motion amplitude, frequency and number of cycles [11].

The mechanical environment at the head-neck junction is complex and is subjected to forces and frictional moments. These vary with time, type of physical activity, characteristics of the patient and implant geometric and material properties [12-14]. Due to its complexity, *in vitro* studies mostly apply the loads in a simplified, two degree of freedom (DoF) system, commonly sliding tests with a representative vertical load as the most important component of the resultant load [15-17].

Studies have reported that frictional moment can also contribute to the fretting corrosion of modular head-neck interface. Panagiotidou et al. [17] reported that increasing the unidirectional frictional torque on the neck axis (0 Nm, 9 Nm, 14 Nm, and 18 Nm) increases the depassivation current of the interface significantly. Jauch et al. [18] monitored the disruption of the passive oxide layer due to the applied torque about the head-neck axis; and therefore, initiation of fretting corrosion. They reported that with an increase in the assembly force of the taper junction from 4.5 kN to 6 kN, the fretting corrosion initiation torque increased from 3.92 ± 0.97 Nm to 7.23 ± 0.55 Nm. In another study, Jauch et al. [19] investigated the overall micro-motion in different head-neck combinations subjected to a unidirectional sinusoidal loading with a maximum magnitude occurring during walking (2.3 kN), stair climbing (4.3 kN) and stumbling (5.3 kN). The micro-motions varied between 3.3 µm and 33.4 µm and increased with rising the peak forces.

To better understand fretting at the head-neck junction, the mechanical environment of the junction needs to be studied in terms of contact pressure, contact length and relative micro-motions. Finite element analysis (FEA) is found to be a cost effective method for this purpose [20, 21]. Fallahnezhad et al. [22] developed a three dimensional finite element (FE) model to investigate the torsional strength of a head-neck taper junction with different material combinations. They reported that under the same assembly force, a greater contact length shapes between a CoCr head and titanium neck compared to a CoCr head and CoCr neck, and consequently the CoCr/Ti combination had a higher torsional strength. Donaldson et al. [21] developed a stochastic FEA to evaluate the effective parameters on the frictional work over a cycle (fretting work) in a head-neck taper junction based on the forces of level gait. They concluded that the major parameters that effectively contribute to the value of fretting work are taper angle mismatch, centre offset and body weight. It was also reported that every 0.1˚ increase in the mismatch angle can increase the contact pressure by 85 MPa. To verify their model, they applied an assembly force at 45˚ off-axis to two sets of head-neck junction made of Al 6061 at a 3:1 size scale. As raised in their paper, for a single case study (not stochastic) a more accurate validation is required for realistic predictions. Dyrkacz et al. [23] developed a 3D FE model to seek the parameters that can affect relative micro-motions in the taper junction. Their study revealed that assembly force, taper size and materials combination play an important role in changing the micro-motion values. However, in their model, the angular mismatch between the head and neck components was neglected while it has a significant effect on the contact pressure and micro-motions [21].

In addition to the previously available contact forces [12, 24, 25], head-cup frictional moments have recently become available for walking activity [26, 27]. This provides 6 DoF load inputs including three force components and three moment components [26]. However, the contribution of the frictional moments to the stress field, relative displacements between the contacting surfaces and consequently fretting wear behaviour has not been reported yet.

Benefiting from the available 6 DoF load inputs, in this study, a finite element analysis of a head-neck taper junction of an implant was conducted in three different loading conditions which include

level walking gait forces only (F only), level walking frictional moments only (M only) and combined gait forces and frictional moments (F&M). This was to carefully evaluate the contribution of frictional moments to the fretting wear related parameters at the interface. The results of this study present a perspective of dynamic stress field and micro-motion at the head-neck interface of the modelled geometry and materials during level gait.

2. Methods

A previously established and verified three dimensional (3D) finite element model of an isolated head-neck junction [22] was further developed to simulate and apply currently available 6 DoF load inputs of level gait. The model consisted of a 12/14 taper design having a 32 mm diameter CoCr head and a CoCr neck with a proximal angular mismatch (head taper angle = 2.858˚, neck taper angle = 2.834˚, angular mismatch = 0.024˚ [28]). The nodes located at the external surface of the head were constrained in all directions. The assembly force (4 kN) and the load components of level gait were applied to the bottom face of the neck. The forces were obtained from Hip98 software [12] and the frictional moments were calculated from a previous study for a 32 mm metal-on-metal bearing couple [26], as shown in Figure 1a. The maximum magnitude of the frictional moments in this 32 mm metal-on-metal bearing (with a friction coefficient of 0.20) was found to be 3.68 Nm. For comparison purposes, the average of maximum frictional moments from 10 patients with a 32 mm ceramic-on-polyethylene bearing was reported as 2.15 Nm with a maximum friction coefficient of 0.19. The highest individual moment was also reported as 4.28 Nm [29]. This indicates that the frictional moments used in the present work are comparable to the available *in-vivo* measurements with similar maximum friction coefficients; however, material combination for the head-neck interface can of course influence the fretting wear related parameters in the junction.

Both the gait force and frictional moment components were sampled over 100% of a normalized gate cycle (0 for initial contact and 100 for terminal swing) and were applied to the end-of-neck coordinate system. The selection of a metal-on-metal bearing for this study was because of their high failure rates together with wear debris and metal ions generation at the head-neck interface [30, 31], and higher frictional moments in comparison with common metal-on-polyethylene bearings [13, 32].

Using ABAQUS/Explicit, an explicit (dynamic) FE analysis was used in this study. A fixed mass-scaling method was applied to reduce the computational time, and the kinetic-energy/total-energy ratio was monitored to be less than 10% during the entire simulations. This assures that inertia forces do not influence the results due to mass-scaling. To simulate mechanical interactions at the head-neck interface, a surface-to-surface discretization contact method with a finite sliding formulation was used. Contact pressures (Cp) were monitored using a Lagrange multiplier formulation. A friction coefficient of 0.3, which was verified previously for the same junction [22], was used in the penalty method for the contact model.

Quadratic tetrahedral elements (C3D10M in ABAQUS) were used to mesh the head and neck models (Figure 1b). The elements were refined in successive steps to achieve mesh-independent results. The size of elements at the contacting interface was 0.15 mm. The head and neck models were meshed with

177,573 and 114,761 elements, respectively. The CoCr alloy (ISO 5238–12) was modelled with an elastic-linear plastic material model with properties of: Young's modulus=210 GPa, Poisson's ratio=0.30, yield strength = 910 GPa, linear-plastic-slope/elastic-modulus = 1.4%, ultimate tensile strength = 1,350 MPa and elongation = 15%.

In the first step, the assembly process of the head-neck junction was replicated for which a force of 4 kN was applied with a rate of 500 N/s. In the second step, the load components of a full gait cycle of normal walking were applied to the bottom face of the neck in three different loading scenarios of: F only (only gait forces), M only (only frictional moments) and F&M (gait forces and frictional moments). Contact pressures (Cps) and micro-motions (δ) were monitored before and after applying the activity gait loads and the time step at which the maximum of contact pressure and micro-motion occurred was determined. It was found that the maximum contact pressure and maximum micro-motion occur simultaneously under the peak force (resultant of F_x, F_y and F_z) for F only and peak frictional moment (resultant of M_x, M_y and M_z) for M only loading scenarios. In the F&M loading case, the maximum contact pressure and maximum micro-motion occurred under the peak force indicating that the force components were more dominant than the moment components in inducing maximum contact pressure and micro-motion.

Using a custom written Python code, the results of contact pressures, shear stresses and displacements were extracted for each loading scenario for all the nodes of the head and neck contacting surfaces at the maximum force and moment instance which resulted in maximum stresses and micro-motions over the gait cycle. A MATLAB code was then implemented to determine micro-motions (relative displacements) and fretting work at the contacting nodes of the head-neck interface for this instance of time. For a better presentation of results, the neck circumference was projected onto a plane and the extracted parameters were presented as the normal axis (z). In this configuration, as shown in Figure 2, the proximal end of the neck was considered as the origin (zero) for the neck length axis. The second axis presents the angular position starting from the middle line of the inferomedial sector (zero radians).

3. Results & Discussion

The results of the mechanical response of the head-neck interface in the form of contact pressure, micro-motions, shear stresses and fretting work are presented and discussed in the following sections. It is then followed by the possible implications of the results for *in vitro* testing.

3.1 Contact pressure

Contact pressures (Cp) are plotted over the neck surface for the three loading scenarios in Figure 3. The contact pressure contours distinguish contacting nodes from non-contacting ones over the neck surface (i.e. non-contacting nodes have zero contact pressure). The assembly force results in a press-fit connection in the proximal side of the junction inducing large local contact pressures (900 MPa at the circular edge). In the M only loading case, the contact area was similar to the initial press-fit area in the proximal region (only 0.27% of the non-contacting surface nodes temporarily came into contact). When subjected to the level gait forces in both the F only and F&M loading cases, the contacting region was extended over the superolateral sector where 8.43% and 9.57% of the initially non-contacting surface

nodes were in contact, respectively. This caused a reduction in the peak Cp in the proximal contact region. The extended contact region in the superolateral sector under the F only and F&M loading cases was due to the bending effect of the force components which suggests that the vertical component of the force was dominant in bending the neck towards the head surface and causing them to contact each other. This occurred while the torsional components of the frictional moment and tangential components of the force with respect to the neck axis lead to relative displacements in the tangential direction of the contacting surface. On the proximal side, the maximum Cps (red circles in Figure 3a-c) were distributed over the initial press-fit area for all the three cases. In the temporary contact region of F only and F&M, the maximum Cps occurred mostly along the middle-line of the superolateral sector. Comparing the maximum magnitudes of contact pressure over the length of the neck (Figure 3d), M only induced the lowest values of Cp in the initial press-fit area (proximal) and negligible contact extension occurred in the remaining length of the neck. Whereas, F only and F&M had similar values of maximum Cp over the neck length. At the proximal press-fit rim, the initial uniform distribution of Cp was disturbed and higher magnitudes occurred at the anterior, posterior and inferomedial sections in F only and F&M loading cases, while this did not significantly change for the M only loading.

3.2 Micro-motions

Figure 4 illustrates the distribution of micro-motion (δ) for the contacting nodes under three cases of loading. Magnitudes of micro-motion for M only were significantly smaller (by order of 10^2) than F only and F&M loading cases. However, the frictional moment increased the micro-motions of the F&M loading compared to the F only case, especially when approaching the distal side of the neck, increasing the most distal micro-motions from 31 to 38 μm. Considering Figure 4a and 4c, the entire contacting area in the F only and F&M loadings experienced similar magnitudes of micro-motions. A similar pattern for the distribution of micro-motions in M only (with peaks in the proximal anterior and posterior sectors) was observed in F only and F&M but with higher magnitudes (by order of 10^2). Although the δ magnitudes for the M only case were negligible, by comparing the maximum values of micro-motion for F only and F&M (Figure 4d), one can find that the superposition of the frictional moments with the gait forces has increased the micro-motions along the neck length.

3.3 Shear stresses

Biometals such as CoCr alloys and Ti alloys offer a good corrosion resistance by forming a thin passive oxide layer with an approximately 10 nm thickness [33]. These oxide layers have low shear strengths [33]; for instance, shear strength of the oxide layer in Ti alloys is less than 40 MPa [34]. Maximum shear stresses along the neck length are plotted in Figure 5. Shear stresses in the proximal initial press-fit region for all the studied loading cases are found to be significantly higher than the shear strength of typical passive oxide layers. Shear stresses of F only and F&M cases in the temporary contacting area were found to be about the reported disruptive shear stress levels for oxide layers. This may suggest that at each gait of walking activity, the oxide layer can experience depassivation. This is aligned with the results of simplified *in vitro* experiments of fretting corrosion at the head-neck interface which showed depassivation/repassivation at each cycle of loading-unloading [17].

3.4 Fretting work

Fretting work per unit of area (J/m^2) was determined as the product of shear stress and its corresponding micro-motion at each point (Figure 6). It can be found that the M only loading results in

negligible fretting work compared to F only and F&M. F only had similar fretting work to F&M, but was more uniform. In the last three millimeters (13 mm - 16 mm) of the temporary extended contact area, the superposition of M with F in the F&M loading scenario almost doubled the maximum fretting work compared to the F only loading case. Maximum magnitudes of fretting work were concentrated around the middle line of the superolateral sector especially in the proximal press-fit rim. It is therefore believed that this sector may be expected to experience a greater level of fretting wear and consequently more material removal. This is in good agreement with retrieval studies which have reported localised damage in superolateral surfaces and press-fit rims [35, 36].

3.5 Range of contact pressures and micro-motions

Maximum Cp and maximum δ were identified in various circumferential hoops around the neck with 1 mm incremental distances over the neck length. These maximum values where plotted versus their corresponding δ and Cp, respectively (Figure 7). It can be seen that the data points are mostly located in a region with an upper pressure of 275 MPa and an upper micro-motion of 38 µm. Also, for a specific Cp such as 100 MPa, there exists a range of corresponding δ from 0 µm to 35 µm. For a specific δ such as 13 µm, the corresponding contact pressure varies approximately from 20 MPa to 200 MPa.

Table 1 presents the maximum δ and its corresponding Cp; and also, maximum Cp and its corresponding δ along the neck length. In the proximal initial press-fit rim, there were zero micro-motion areas, although their Cps were not higher than those of in the adjacent areas. In other words, higher Cps did not coincide with minimum δs as there were non-zero δs for maximum Cps (Table 1). Considering the influence of contact pressure and micro-motion on the phenomenon of fretting wear, the ranges presented in Figure 7 and Table 1 may provide an indicative guideline for future *in vitro* tests on CoCr/CoCr head-neck junctions (with the same geometry and dimensions reported in this work) to depict a realistic picture of the mechanical environment of these junctions during normal walking activity.

Table 1. Variaiton of contact pressure (Cp) – micromotion (δ) over the neck length for the studied loading cases of F only, M only and F&M. The location of Max Cp and Max δ are specified by "(A)" as anterior, "(P)" as posterior, "(S)" as superolateral and "(I)" as inferomedial sides of the neck.

	F&M				**M only**				**F only**			
Z (mm)	Max. δ (µm)	Cp (MPa)	Max. Cp. (MPa)	δ (µm)	Max. δ (µm)	Cp (MPa)	Max. Cp. (MPa)	δ (µm)	Max. δ (µm)	Cp (MPa)	Max. Cp. (MPa)	δ (µm)
0	19 (P)	662	814.2 (A)	17	0.3 (I)	618.3	874.0 (P)	0.01	12 (P)	659	880.4 (A)	11
1	20 (P)	179	325.6 (P)	19	0.3 (I)	113.2	262.8 (I)	0.01	13 (P)	142	269.5 (A)	1
2	19 (A)	119	185.2 (A)	13	0.6 (A)	544.7	152.5(P)	0.02	12 (P)	46.6	159.4 (A)	1
3	11 (A)	36.1	261.1 (S)	4	-	-	-	-	7 (P)	22.6	182.1 (S)	3
4	5 (S)	139	147.5 (S)	4	-	-	-	-	4 (S)	46.1	119 (A)	3
5	6 (S)	56.7	122.9	6	-	-	-	-	5 (S)	57.8	114.6	3

			(S)								(A)	
6	9 (S)	42.7	115.8 (S)	9	-	-	-	-	8 (S)	37.4	78.4 (S)	8
7	11 (S)	32.1	127.7 (S)	11	-	-	-	-	10 (S)	26.7	88.1 (S)	9
8	13 (S)	30.2	74.4 (S)	13	-	-	-	-	11 (S)	24.9	64.5 (S)	11
9	16 (S)	29.5	68.3 (S)	15	-	-	-	-	13 (S)	18.9	61.8 (S)	13
10	18 (S)	9	76.3 (S)	18	-	-	-	-	15 (S)	10.1	81.7 (S)	15
11	23 (S)	2.2	30.2 (S)	23	-	-	-	-	19 (S)	30.3	44.4 (S)	19
12	26 (S)	5.2	90.1 (S)	2.6	-	-	-	-	22 (S)	11.4	66.1 (S)	21
13	29 (S)	28.8	79.1 (S)	28	-	-	-	-	24 (S)	90.6	90.6 (S)	24
14	31 (S)	20.8	102.4 (S)	31	-	-	-	-	26 (S)	44	108.4 (S)	26
15	34 (S)	5.5	102.2 (S)	34	-	-	-	-	28 (S)	138	137.7 (S)	28
16	37 (S)	16.8	143.4 (S)	37	-	-	-	-	31 (S)	126	198.6 (S)	30

For the modelled geometry and materials, and under the loading of walking activity, this work demonstrate that the force components had a significant influence on the stress distribution, micro-motions and fretting work. Focusing more on the isolated role of frictional moments in the fretting related characteristics at the interface, the results of this study indicate a negligible effect purely from the frictional moments. However, when the frictional moments are superposed with the forces, they intensify the mechanical response of the interface, especially in terms of fretting work.

It is noted that this work is limited to fretting wear related parameters (contact stresses and relative micro-motions) and does not study the electrochemical behaviour of the head and neck materials. However, as mentioned in the introduction, fretting wear is the initiator/assistant of corrosion within the crevice of the junction (mechanically assisted crevice corrosion). The fretting wear related results of this finite element study can only indicatively assist the interpretation of implant retrieval studies, especially the ones with similar taper geometries and materials. Given that both fretting wear and corrosion are sensitive to the geometry of the interface [37, 38], one should be cautious expanding the results of this work to the other geometries and materials. Instead, the finite element modelling approach developed in this work can be applied to the other materials and taper geometries (e.g. various taper angle mismatches, and head diameters) in order to use their results more accurately for future relevant *in vitro* studies.

4. Conclusions

The effects of realistic loads (level gait forces and frictional moments - F&M) of walking activity on the mechanical response of the head-neck interface in hip implants were studied. For understanding the level of contribution of the frictional moments to the mechanical response of the interface, two additional loading scenarios of gait forces only (F only) and frictional moments only (M only) were also studied. A 3D finite element model was developed to analyse a CoCr/CoCr junction with a head size of 32 mm having a 12/14 taper design and a proximal mismatch angle of 0.024° which was initially assembled with a 4 kN force. The simulations were performed to obtain stress field, micro-motions and fretting work for this taper junction under a complex 6 degree of freedom loading during a gait cycle of walking. Normal contact stresses and micro-motions at the interface were mostly found in the ranges of 0-275 MPa and 0-38 µm, respectively. The frictional moments alone had a negligible effect in increasing the contacting area as only 0.27% of the non-contacting surface nodes were engaged in contact. F only made 8.43% of the non-contacting surface nodes to get in contact. Frictional moments were effective in the F&M case as the contacting nodes increased to 9.57% when compared to 8.43% in the F only case. Superposition of the frictional moments and gait forces (F&M) in comparison with F only, also resulted in:

a) Up to an approximately 100% increase in the maximum value of fretting work per unit area in the last three millimeters of the temporary extended contacting area (14mm- 16mm).
b) An approximately 15% increase in the maximum magnitude of micro-motions.

The results suggest that gait forces dominate the mechanical environment of the interface; however frictional moments when combined with the gait forces can have some considerable effects on increasing the fretting work and gradually increasing micro-motions in the contacting area. This may suggest that simplifying mechanical loads of daily activities to gait forces only in both finite element and *in vitro* studies needs acceptable justifications.

Conflict of interest statement

The authors declare that there is no conflict of interest.

Acknowledgments

The authors would like to acknowledge the support through an Australian Government Research Training Program Scholarship for Mr Hamidreza Farhoudi's and Mr Khosro Fallahnezhad's PhD studies.

References

1. Krishnan, H., et al., *INSTRUCTIONAL REVIEW: HIP Modular neck femoral stems.* The bone and joint journal, 2013. **95**: p. 1011-1021.
2. Hussenbocus, S., et al., *Head-Neck Taper Corrosion in Hip Arthroplasty.* BioMed Research International, 2015. **2015**: p. 9.
3. Korovessis, P., et al., *Metallosis after contemporary metal-on-metal total hip arthroplasty: Five to nine-year follow-up.* Journal of Bone and Joint Surgery - Series A, 2006. **88**(6): p. 1183-1191.
4. Hart, A.J., et al., *The chemical form of metallic debris in tissues surrounding metal-on-metal hips with unexplained failure.* Acta Biomaterialia, 2010. **6**(11): p. 4439-4446.
5. Huber, M., et al., *Presence of corrosion products and hypersensitivity-associated reactions in periprosthetic tissue after aseptic loosening of total hip replacements with metal bearing surfaces.* Acta Biomater, 2009. **5**(1): p. 172-80.
6. Hart, A.J., et al., *Circulating levels of cobalt and chromium from metal-on-metal hip replacement are associated with CD8+ T-cell lymphopenia.* J Bone Joint Surg Br, 2009. **91**(6): p. 835-42.
7. Cooper, H.J., et al., *Corrosion at the head-neck taper as a cause for adverse local tissue reactions after total hip arthroplasty.* J Bone Joint Surg Am, 2012. **94**(18): p. 1655-61.
8. Higgs, G.B., et al., *Is increased modularity associated with increased fretting and corrosion damage in metal-on-metal total hip arthroplasty devices?: a retrieval study.* J Arthroplasty, 2013. **28**(8 Suppl): p. 2-6.
9. Bryant, M., *Fretting-crevice corrosion of cemented metal on metal total hip replacements*, in *School of Mechanical Engineering*. 2013, The University of Leeds.
10. Swaminathan, V. and J.L. Gilbert, *Fretting corrosion of CoCrMo and Ti6Al4V interfaces.* Biomaterials, 2012. **33**(22): p. 5487-5503.
11. Berthier, Y., L. Vincent, and M. Godet, *Fretting fatigue and fretting wear.* Tribology International, 1989. **22**(4): p. 235-242.
12. Bergmann, G., et al., *Realistic loads for testing hip implants.* Bio-Medical Materials and Engineering, 2010. **20**(2): p. 65-75.
13. Bishop, N.E., F. Waldow, and M.M. Morlock, *Friction moments of large metal-on-metal hip joint bearings and other modern designs.* Medical Engineering & Physics, 2008. **30**(8): p. 1057-1064.
14. Farhoudi, H., et al., *A novel analytical approach for determining the frictional moments and torques acting on modular femoral components in total hip replacements.* Journal of Biomechanics, 2015. **48**(6): p. 976-983.
15. Gilbert, J.L., M. Mehta, and B. Pinder, *Fretting crevice corrosion of stainless steel stem–CoCr femoral head connections: Comparisons of materials, initial moisture, and offset length.* Journal of Biomedical Materials Research Part B: Applied Biomaterials, 2009. **88B**(1): p. 162-173.
16. Goldberg, J.R. and J.L. Gilbert, *In vitro corrosion testing of modular hip tapers.* Journal of Biomedical Materials Research Part B: Applied Biomaterials, 2003. **64B**(2): p. 78-93.
17. Panagiotidou, A., et al., *The effect of frictional torque and bending moment on corrosion at the taper interface : an in vitro study.* Bone Joint J, 2015. **97-b**(4): p. 463-72.
18. Jauch, S.Y., et al., *Low torque levels can initiate a removal of the passivation layer and cause fretting in modular hip stems.* Medical Engineering & Physics, 2014. **36**(9): p. 1140-1146.
19. Jauch, S., et al., *MICRO-MOTIONS AT THE STEM-HEAD TAPER OF MODULAR HIP PROSTHESES DURING DAILY LIVING ACTIVITIES.* Orthopaedic Proceedings, 2016. **98-B**(SUPP 8): p. 59-59.
20. English, R., A. Ashkanfar, and G. Rothwell, *A computational approach to fretting wear prediction at the head–stem taper junction of total hip replacements.* Wear, 2015. **338–339**: p. 210-220.

21. Donaldson, F.E., J.C. Coburn, and K.L. Siegel, *Total hip arthroplasty head–neck contact mechanics: A stochastic investigation of key parameters.* Journal of Biomechanics, 2014. **47**(7): p. 1634-1641.
22. Fallahnezhad, K., et al., *Influence of geometry and materials on the axial and torsional strength of the head–neck taper junction in modular hip replacements: A finite element study.* Journal of the mechanical behavior of biomedical materials, 2016. **60**: p. 118-126.
23. Dyrkacz, R.M.R., et al., *Finite element analysis of the head–neck taper interface of modular hip prostheses.* Tribology International, 2015. **91**: p. 206-213.
24. Bergmann, G., F. Graichen, and A. Rohlmann, *Hip joint loading during walking and running, measured in two patients.* Journal of Biomechanics, 1993. **26**(8): p. 969-990.
25. English, T.A. and M. Kilvington, *In vivo records of hip loads using a femoral implant with telemetric output (a prelimary report).* Journal of Biomedical Engineering, 1979. **1**(2): p. 111-115.
26. Farhoudi, H., et al., *An Analytical Calculation of Frictional and Bending Moments at the Head-Neck Interface of Hip Joint Implants during Different Physiological Activities.* Materials, 2016. **9**(12): p. 982.
27. Damm, P., et al., *Friction in Total Hip Joint Prosthesis Measured In Vivo during Walking.* PLoS ONE, 2013. **8**(11): p. e78373.
28. Rehmer, A., N.E. Bishop, and M.M. Morlock, *Influence of assembly procedure and material combination on the strength of the taper connection at the head–neck junction of modular hip endoprostheses.* Clinical Biomechanics, 2012. **27**(1): p. 77-83.
29. Damm, P., et al., *In vivo measured joint friction in hip implants during walking after a short rest.* PLOS ONE, 2017. **12**(3): p. e0174788.
30. Cook, R.B., et al., *Pseudotumour Formation Due to Tribocorrosion at the Taper Interface of Large Diameter Metal on Polymer Modular Total Hip Replacements.* The Journal of Arthroplasty, 2013. **28**(8): p. 1430-1436.
31. Bolland, B.J.R.F., et al., *High failure rates with a large-diameter hybrid metal-on-metal total hip replacement: clinical, radiological and retrieval analysis.* Journal of Bone & Joint Surgery, British Volume, 2011. **93-B**(5): p. 608-615.
32. Flanagan, S., E. Jones, and C. Birkinshaw, *In vitro friction and lubrication of large bearing hip prostheses.* Proc Inst Mech Eng H, 2010. **224**(7): p. 853-64.
33. Bronzino, J., *Biomedical Engineering Fundamentals*. 2006: CRC Press.
34. Liu, X., P.K. Chu, and C. Ding, *Surface modification of titanium, titanium alloys, and related materials for biomedical applications.* Materials Science and Engineering: R: Reports, 2004. **47**(3–4): p. 49-121.
35. Higgs, G.B., et al., *Is Increased Modularity Associated With Increased Fretting and Corrosion Damage in Metal-On-Metal Total Hip Arthroplasty Devices?: A Retrieval Study.* The Journal of arthroplasty, 2013. **28**(8 0): p. 2-6.
36. Kurtz, S.M., et al., *Do Ceramic Femoral Heads Reduce Taper Fretting Corrosion in Hip Arthroplasty? A Retrieval Study.* Clinical Orthopaedics and Related Research, 2013. **471**(10): p. 3270-3282.
37. Bryant, M., et al., *Characterisation of the surface topography, tomography and chemistry of fretting corrosion product found on retrieved polished femoral stems.* Journal of the Mechanical Behavior of Biomedical Materials, 2014. **32**(0): p. 321-334.
38. Neu, R.W., *Progress in standardization of fretting fatigue terminology and testing.* Tribology International, 2011. **44**(11): p. 1371-1377.

Figures:

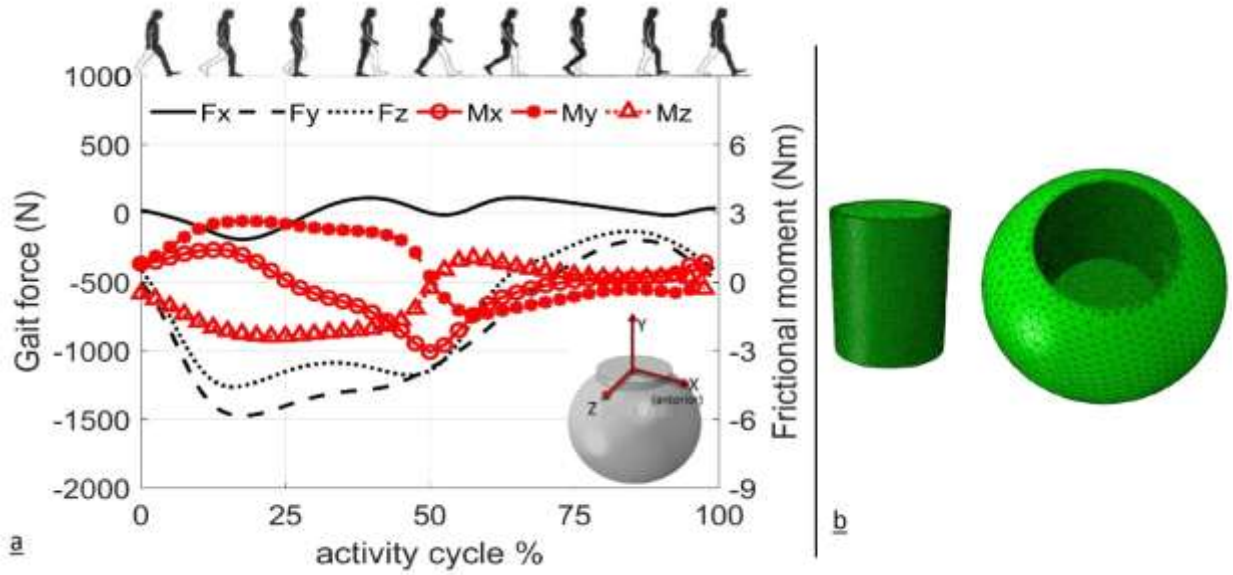

Figure 1. (a) Input gait forces and frictional moments for a normalized walking gait cycle presented in a coordinate system at the bottom face of the neck (end-of-neck coordinate system) for right hip, and (b) finite element models of head and neck with a meshing structure gradually refined towards the contact interface.

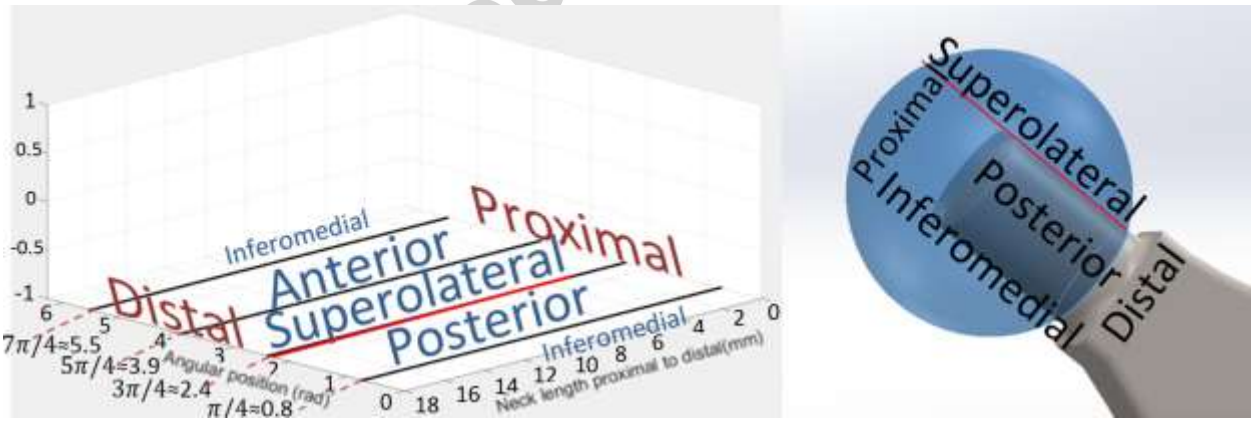

Figure 2. 3D configuration used for results presentation.

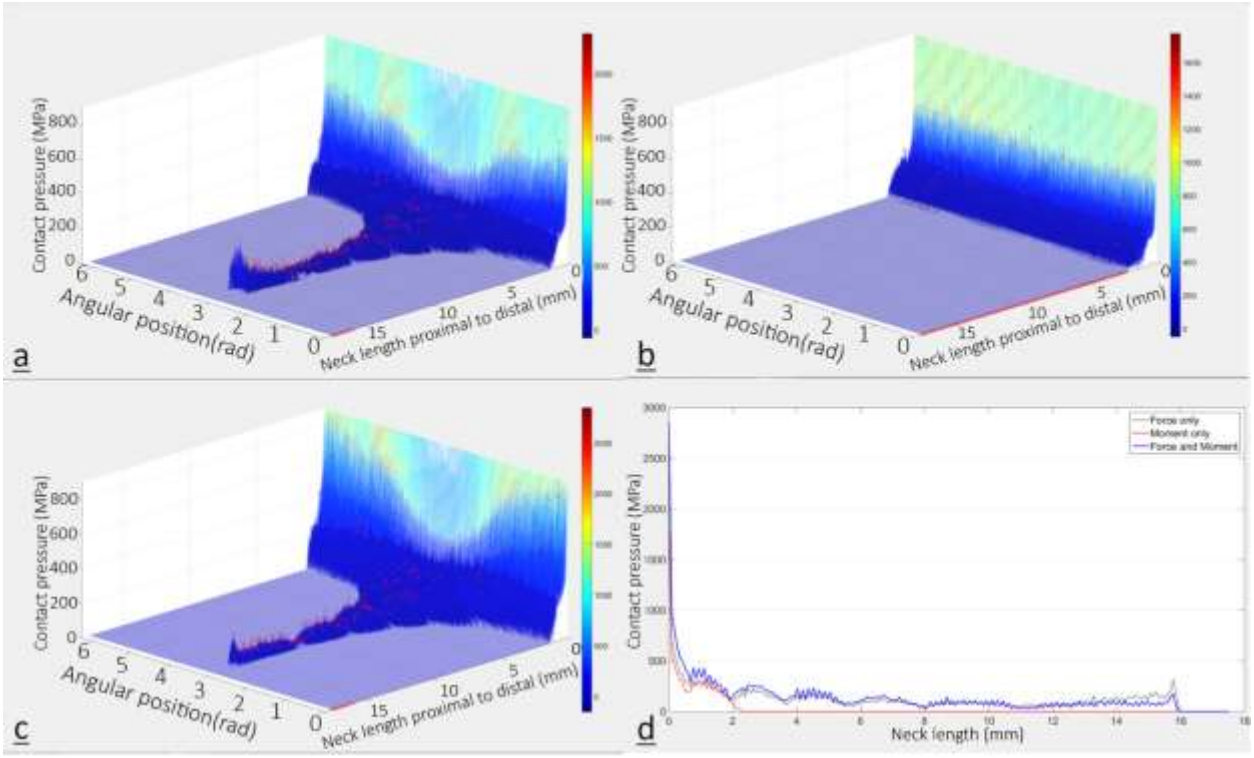

Figure 3. Distribution of contact pressure (Cp) in MPa over the neck surface for: (a) force only, (b) moment only, (c) force and moment loading scenarios. Small red circles in the contours indicate the maximum contact pressure in each division of the neck length over 360 degrees of the neck circumference, and (d) maximum magnitudes of contact pressure along the neck length.

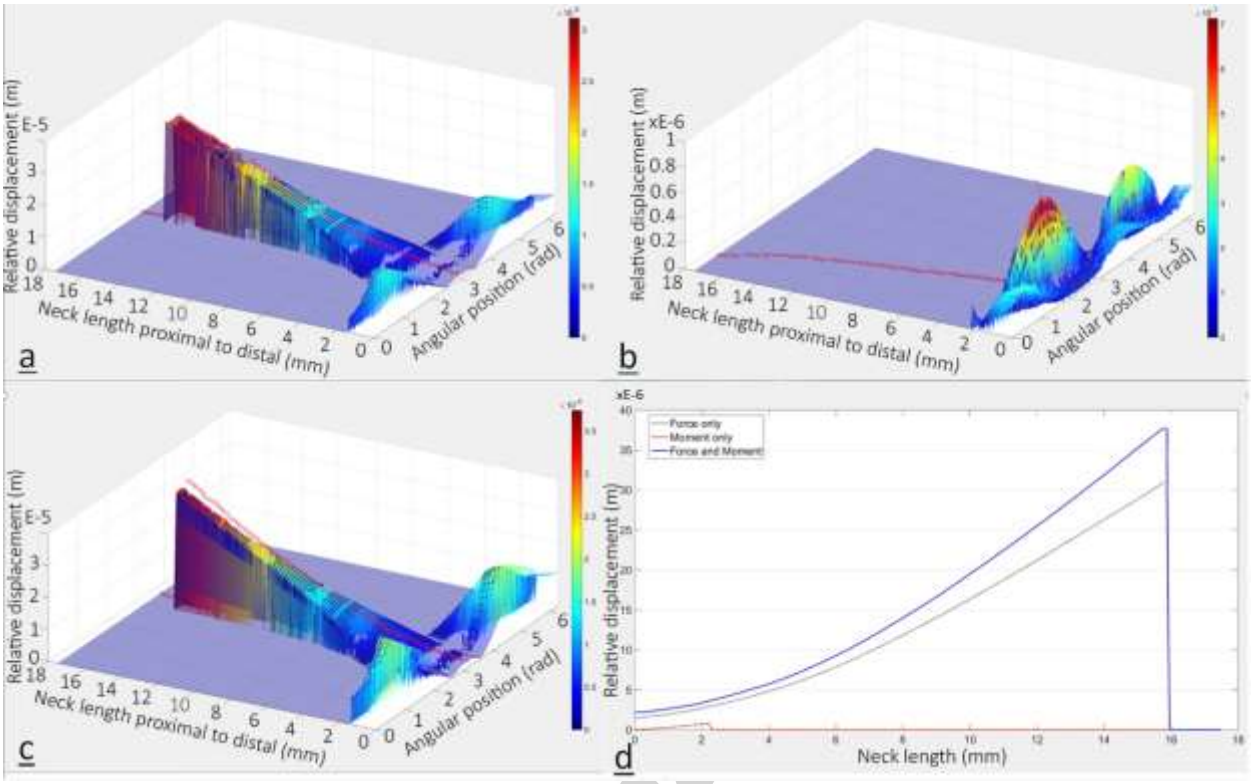

Figure 4. Distribution of relative micro-motions for contacting nodes for: (a) force only loading, (b) moment only loading, (c) force and moment loading, and (d) maximum magnitudes of micro-motion along the neck length.

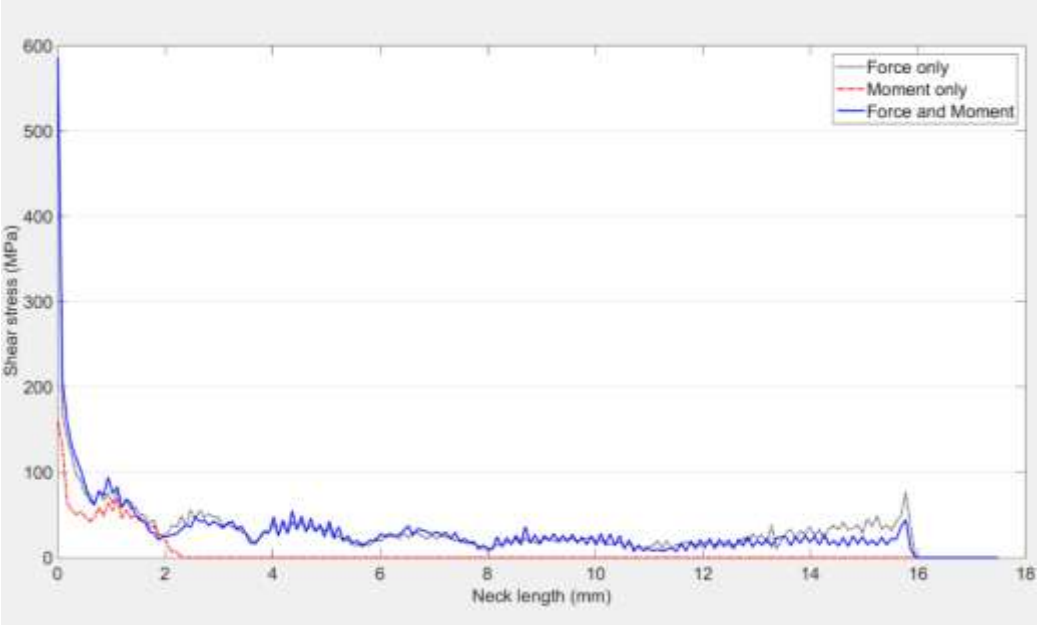

Figure 5. Maximum Shear stress distribution along the neck axis for three cases of loading.

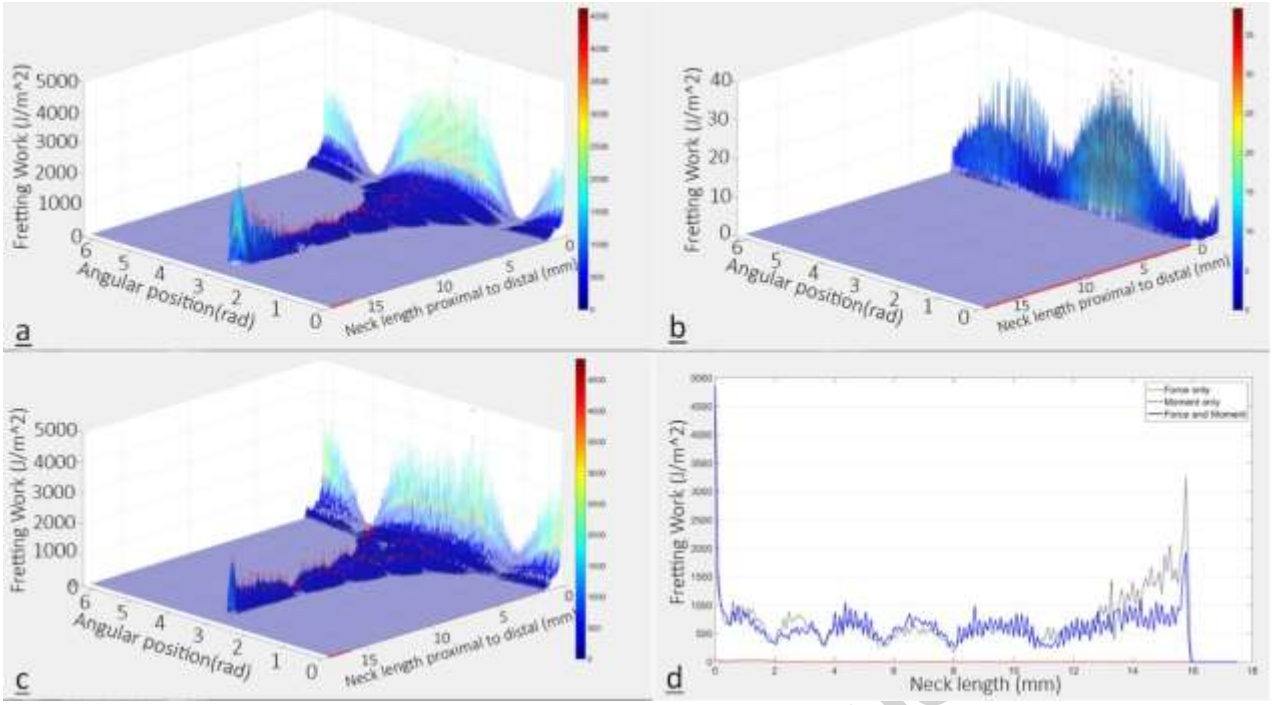

Figure 6. Fretting work per unit of area: (a) force only loading, (b) moment only loading, (c) force and moment loading, and (d) maximum magnitudes of fretting work along the neck axis.

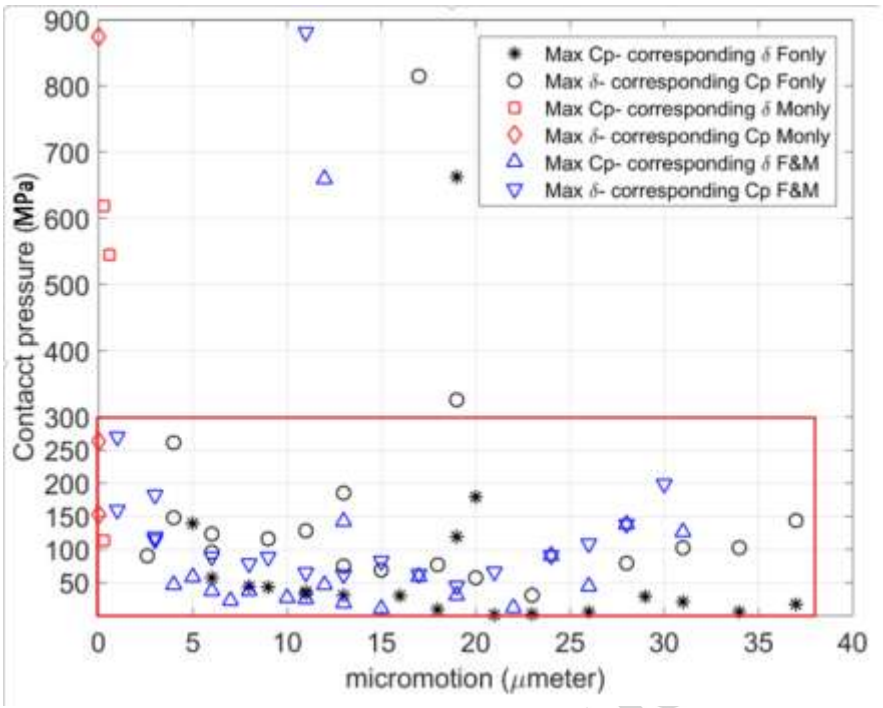

Figure 7. Maximum contact pressures and their corresponding micro-motions, and maximum micro-motions and their corresponding contact pressures over the neck circumference and in 1mm intervals for studied loading cases of F only, M only and F&M.

Highlights

- A FE study on the mechanical response of a CoCr/CoCr taper junction in hip implants
- Three loading scenarios of walking gait forces, moments and combined were studied
- The contact pressure distribution was extended over the superolateral sector
- Compared to moments, forces dominantly increased contact pressure and micro-motions
- Micro-motion and contact pressure varied between 0-38 µm and 0-275 MPa respectively